INVESTIGATOR'S BROCHURE For:

[^{18}F]FLUOROMISONIDAZOLE, 1H-1-(3-[^{18}F]-FLUORO-2-HYDROXY-PROPYL)-2-NITRO-IMIDAZOLE, [^{18}F]FMISO

AN INVESTIGATIONAL POSITRON EMISSION TOMOGRAPHY (PET) RADIOPHARMACEUTICAL FOR INJECTION AND INTENDED FOR USE AS AN IN VIVO DIAGNOSTIC FOR IMAGING HYPOXIA IN TUMORS.

Investigational New Drug (IND) Application

IND # 76,042

Your name and address goes here

Edition Number: 4
Approval Date: 11/09/2009

I. TABLE OF CONTENTS 2

II. [^{18}F]FMISO PRODUCT AGENT DESCRIPTION 3

1. AGENT DESCRIPTION 3
2. CHEMICAL STRUCTURE 3
3. FINAL PRODUCT SPECIFICATIONS 4

III. INTRODUCTION 5

IV. PHARMACOLOGY 6

1. PHYSICAL CHARACTERISTICS 6
2. MECHANISM OF ACTION 6

V. TOXICOLOGY AND SAFETY 6

1. MECHANISM OF ACTION FOR TOXICITY 6
2. FMISO CELL TOXICITY STUDIES 10
3. ANIMAL TOXICITY STUDIES: MISO AND FMISO 11
4. HUMAN TOXICITY STUDIES: MISO 12
5. [^{19}F]FMISO HUMAN TOXICITY 13
6. [^{18}F]FMISO HUMAN TOXICITY 14
7. MISO HUMAN SAFETY STUDIES 14
8. [^{19}F]FMISO HUMAN SAFETY STUDIES 15
9. [^{18}F]FMISO HUMAN SAFETY STUDIES 15
10. FMISO GENOTOXICITY AND MUTAGENICITY 16
11. ADVERSE EVENTS AND MONITORING FOR TOXICITY 16
12. SAFETY AND TOXICITY OF THE OTHER COMPONENTS OF THE FINAL [^{18}F]FMISO DRUG PRODUCT 17

VI. BIODISTRIBUTION AND RADIATION DOSIMETRY OF FMISO 18

VII. [^{18}F]FMISO PREVIOUS HUMAN EXPERIENCE AND ASSESSMENT OF CLINICAL POTENTIAL 23

VIII. REFERENCES 30

TABLE OF TABLES

Table 1. Final Product Components per single injected dose 4
Table 2. Final Product Impurities per single injected dose 4
Table 3. Final Product Specifications 5
Table 4. Biodistribution of [^{3}H]fluoromisonidazole in C3H mice32 9
Table 5. Inhibition of [^{3}H]FMISO Binding by Oxygen *in vitro* 11
Table 6. Clinical toxicity of misonidazole 13
Table 7. Radiation Absorbed Dose to Organs 22
Table 8. Published manuscripts reporting ^{18}F-FMISO human imaging studies 26

TABLE OF FIGURES

Figure 1. The chemical structure of [^{18}F]-fluoromisonidazole 3
Figure 2. Metabolism of 2-nitroimidazoles 7
Figure 3. FMISO blood and tissue clearance curves in a dog with osteosarcoma 10
Figure 4. Activity of FMISO in 4 source organs 19
Figure 5. Activity of FMISO in four other source organs 20
Figure 6. Bladder activity 21
Figure 7. Right-frontal glioma post surgery. 29

II. [^{18}F]FMISO PRODUCT AGENT DESCRIPTION

1. AGENT DESCRIPTION

Fluorine-18 labeled misonidazole, 1H-1-(3-[^{18}F]-fluoro-2-hydroxy-propyl)-2-nitro-imidazole, or [^{18}F]FMISO, is a radiolabeled imaging agent that has been used for investigating tumor hypoxia with positron emission tomography (PET). The University of Washington pioneered the development and biodistribution evaluation of [^{18}F]FMISO. An ideal hypoxia-imaging agent should distribute independently of blood flow, which is best achieved when the partition coefficient of the tracer is close to unity. Under these circumstances, imaging can be done at a time when the intracellular tracer distribution has equilibrated with the tracer in plasma near the cells. [^{18}F]FMISO is an azomycin-based hypoxic cell sensitizer that has a nearly ideal partition coefficient and, when reduced by hypoxia, binds covalently to cellular molecules at rates that are inversely proportional to intracellular oxygen concentration, rather than by any downstream biochemical interactions.[1]

2. CHEMICAL STRUCTURE

[^{18}F]FMISO has not been marketed in the United States and, to the best of our knowledge, there has been no marketing experience with this drug in other countries. The radiopharmaceutical product, [^{18}F]FMISO is the only active ingredient and it is dissolved in a solution of ≤10 mL of 95% isotonic saline 5% ethanol (v:v). The drug solution is stored in at room temperature in a gray butyl septum sealed, sterile, pyrogen-free glass vial with an expiration time of 12 hours. The injectable dose of [^{18}F]FMISO for most studies will be ≤ 10 mCi of radioactive ^{18}F at a specific activity of greater than 125 Ci/mmol at the time of injection. In the dose of [^{18}F]FMISO only a small fraction of the FMISO molecules are radioactive. The amount of injected drug is ≤ 15 µg (≤ 80 nmol per dose) of FMISO. [^{18}F]FMISO is administered to subjects by intravenous injection of ≤ 10 mL.

There is no evidence that nonradioactive and radioactive FMISO molecules display different biochemical behavior.

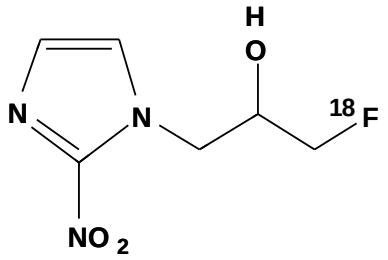

Figure 1. The chemical structure of [^{18}F]-fluoromisonidazole
1H-1-(3-[^{18}F]-fluoro-2-hydroxy-propyl)-2-nitro-imidazole

3. FINAL PRODUCT SPECIFICATIONS

The name of the drug is 1H-1-(3-[^{18}F]-fluoro-2-hydroxy-propyl)-2-nitro-imidazole, or [^{18}F]-fluoromisonidazole, ([^{18}F]FMISO). FMISO is the only active ingredient and it is formulated in a solution of ≤10 mL of 95% 0.15 M saline: 5% ethanol (v:v). The drug product is stored at room temperature in a gray butyl septum sealed, sterile, pyrogen-free glass vial with an expiration time of 12 hours. The injectable dose of [^{18}F]FMISO is ≤ 0.10 mCi/kg not to exceed 10 mCi with a specific activity greater than 125 Ci/mmol at the time of injection. The amount of injected drug is ≤ 15 μg (≤ 80 nmol) of FMISO. [^{18}F]FMISO is administered to subjects by intravenous injection of ≤10 mL. In the dose of [^{18}F]FMISO, only a small fraction of the FMISO molecules are radioactive. There is no evidence that nonradioactive and radioactive FMISO molecules display different biochemical behavior.

The product components are listed in Table 1, the impurities in Table 2, and the final product specifications in Table 3

Table 1. Final Product Components per single injected dose

COMPONENTS	Characterization	Amount in Injectate
[^{18}F]FMISO, 1H-1-(3-[^{18}F]-fluoro-2-hydroxy-propyl)-2-nitro-imidazole	Same as for [^{19}F]FMISO	≤ 10 mCi
[^{19}F]FMISO, 1H-1-(3-[^{19}F]-fluoro-2-hydroxy-propyl)-2-nitro-imidazole	NCS#292930	≤ 15 μg
Ethanol, absolute	USP	5% by volume
Saline for injection	USP	0.15 M

Table 2. Final Product Impurities per single injected dose

IMPURITIES	Acceptance Criteria	Highest Values in 9 Qualification Runs
Kryptofix® [2.2.2]	< 50 μg/mL	None detected
Acetonitrile	< 400 ppm	< 50 ppm
Acetone	< 5000 ppm	< 313 ppm
Other UV absorbing impurities	≤ 35 μg	4.9 μg (1 hr post synthesis)

Table 3. Final Product Specifications

TEST	SPECIFICATION
Chemical Purity (particulates)	Clear and Colorless
pH	6-8
Residual Kryptofix® [2.2.2]	< 50 µg/ mL Kryptofix®
Radiochemical Purity (HPLC)	> 95%
Chemical Purity (HPLC)	FMISO ≤ 15 µg per injected dose
	≤ 35 µg per dose other UV absorbing impurities eluted >3 min (327, 280 or 254 nm)
Radiochemical Purity (TLC)	R_f = >0.5 Purity ≥ 95%
Residual Solvent Levels	Acetone < 5000 ppm Acetonitrile < 400 ppm
Radionuclidic Purity	Measured half-life 100-120 minutes
Bacterial Endotoxin Levels	< 175 EU per dose
Sterility	no growth observed in 14 days , must also pass filter integrity test

III. INTRODUCTION

[^{18}F]-fluoromisonidazole ([^{18}F]FMISO) is a radiolabeled imaging agent that has been used for investigating tumor hypoxia with positron emission tomography (PET). [^{18}F] decays by positron emission. FMISO binds covalently to cellular molecules at rates that are inversely proportional to intracellular oxygen concentration. In hypoxic cells, FMISO is trapped, which is the basis for the use of this tracer to measure hypoxia. Because tissue oxygenation may serve as a marker of perfusion, response to radiotherapy and chemotherapy, tumor grade, and prognosis, development of a PET imaging agent for tumor hypoxia is a potentially valuable avenue of investigation.

Positron emission tomography (PET) is a quantitative tomographic imaging technique, which produces cross-sectional images that are composites of volume elements (voxels). In PET images, the signal intensity in each voxel is dependent upon the concentration of the radionuclide within the target tissue (e.g., organ, tumor) volume. To obtain PET imaging data, the patient is placed in a circumferential detector array.

Patients undergo two separate components in a typical PET imaging procedure. One component is a transmission scan via a germanium rod source or, in the case of PET-CT, by CT imaging of the body region(s) of interest. The second component of the study is the emission scan which can be a dynamic imaging acquisition over a specific area of interest, or multiple acquisitions over the whole body. The typical PET study takes about 20 minutes to 2 hours to perform depending upon the nature of the acquisitions and the areas of the body that are imaged.

The [^{18}F]FMISO radiotracer (≤ 10 mCi) is administered by intravenous injection. Imaging can commence immediately upon injection for a fully quantitative study over one area of the body. More often only a static image is acquired for a 20-minute interval beginning between 100 and 150 minutes post injection.

IV. PHARMACOLOGY

1. PHYSICAL CHARACTERISTICS

Fluoromisonidazole is a small, water-soluble molecule with a molecular weight of 189.14 Daltons. It has an octanol:water partition coefficient of 0.41, so that it would be expected to reflect plasma flow as an inert, freely-diffusible tracer immediately after injection, but later images should reflect its tissue partition coefficient in normoxic tissues.

2. MECHANISM OF ACTION

[^{18}F]FMISO is an azomycin-based hypoxic cell sensitizer that has a nearly ideal partition coefficient and, when reduced by hypoxia, binds covalently to cellular molecules at rates that are inversely proportional to intracellular oxygen concentration, rather than by any downstream biochemical interactions[1]. The covalent binding of nitroimidazoles is due to bioreductive alkylation based on reduction of the molecule through a series of 1-electron steps in the absence of oxygen[2]. Products of the hydroxylamine, the 2-electron reduction product, bind stably in cells to macromolecules such as DNA, RNA, and proteins. In the presence of oxygen, a futile cycle results in which the first 1-electron reduction product, the nitro radical anion, is re-oxidized to the parent nitroimidazole, with simultaneous production of an oxygen radical anion. FMISO is not trapped in necrotic tissue because mitochondrial electron transport is absent. The normal route of elimination for FMISO is renal. A small fraction of [^{18}F]FMISO is glucuronidated and excreted through the kidneys as the conjugate.

V. TOXICOLOGY AND SAFETY

1. MECHANISM OF ACTION FOR TOXICITY

Therapeutic Implications of Hypoxia. Tumor physiology differs from that of normal tissue in several significant ways. Circumstances within tumor tissue can result in hypoxia when growth outpaces angiogenesis or when the oxygen demands of accelerated cellular proliferation exceed local oxygen concentrations. Because hypoxia increases tumor radioresistance, it is important to identify patients whose disease poses this risk for therapeutic failure, lest hypoxic cells survive radiotherapy while retaining their potential to proliferate[3,4]. The selectivity of nitroimidazoles for hypoxic conditions has been demonstrated in rat myocytes[5,6], the gerbil stroke model[7,8], pig livers[9,10], rat

livers[11,12] and dog myocardium[13,14], as well as numerous cancer studies in cell cultures, animals and human trials[15,16].

The mechanism of action of FMISO is common to all nitroimidazoles and is based on the chemical reduction that takes place in hypoxic tissue, covalently binding the chemical to macromolecules in that tissue. The specificity of the reaction is enhanced by the fact that both the reduction and the binding occur within the same cell[17,18]. The reduction reaction, depicted in Figure 2, is reversible at the first step, depending upon the oxygenation status of the tissue, so that some FMISO eventually returns to the circulation and is excreted[19]. The reduction of the nitro group on the imidazole ring is accomplished by tissue nitroreductases that appear to be plentiful and therefore do not represent a rate-limiting factor[1]. The 1-electron reduction product (labeled as "II" in Figure 2) may be further reduced to "III" or it may competitively transfer its extra electron to O_2 and thus reform "I." This binding takes place at a rate that is inversely related to cellular oxygen concentration[6].

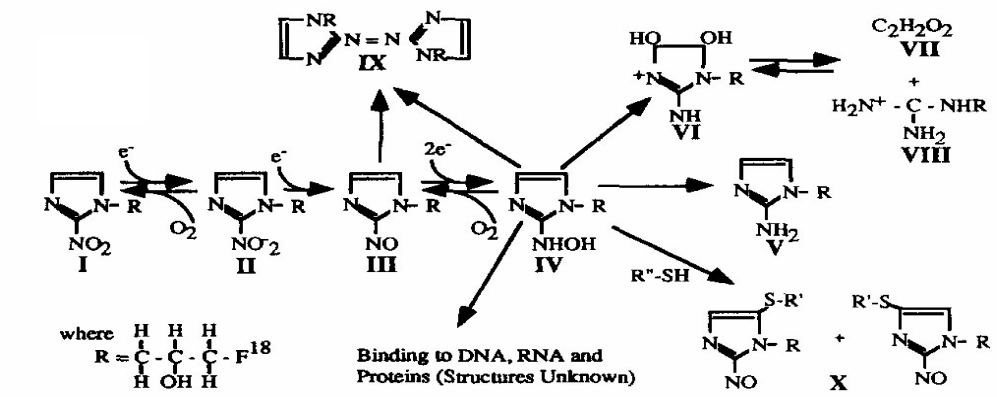

Figure 2. Metabolism of 2-nitroimidazoles.
See text (above figure) for further details

..

Nitroimidazoles bind to hypoxic tissue, serving as hypoxia markers. They potentiate the cytotoxic effects of some chemotherapeutic agents such as the nitrosoureas, melphelan and cyclophosphamide[20,21]. Identifying hypoxic tissue has therapeutic implications for multiple disease states including stroke, myocardial ischemia, and is of particular value in cancer radiotherapy, as hypoxic cancer tissue is relatively radioresistant[22]. These chemical properties suggested the possibility of clinically imaging hypoxic tissue in vivo. Misonidazole, or a related compound, could be labeled with a radioisotope, and could bind to oxygen-deprived cells covalently, providing a positive image of hypoxia via PET. Fluoromisonidazole (Figure 1) has several properties that make it a potentially useful imaging agent. In contrast to the prototype molecule, misonidazole, FMISO can be labeled at the end of the alkyl side chain with ^{18}F, a positron emitter with a 110 minute half-life[23,24]. Fluorine-carbon bonds are highly stable and so the radioactive ^{18}F would be expected to remain on the molecule of interest.

MISO and fluoromisonidazole (FMISO) are 2-nitroimidazoles with nearly identical octanol:water partition coefficients, making them sufficiently lipophilic that they readily diffuse across cell membranes and into tissues[25], yet maintain a volume of distribution essentially equal to total body water[26]. They are less than 5% protein bound, allowing efficient transport from blood into tissues[17]. The distribution kinetics of 2-nitroimidazoles fit a linear two-compartment open model, except that high plasma concentrations after therapeutic level (gram) injections appear to saturate elimination processes in both mice and humans and proceed to non-linear kinetics.

Metabolism and Elimination. *In vitro,* MISO can be reduced using zinc, iron in HCl, xanthine oxidase and NADH[1]. In HeLa and CHO (hamster ovary) cells, reduction appears only under hypoxic conditions. Comparison with MISO indicates that the reduction reaction is similar, but slightly slower for FMISO[1]. FMISO achieves higher tumor:blood and tumor:muscle concentration ratios than MISO in murine tumors[27].

In vivo, under normal oxygen tension, MISO is metabolized primarily in the liver to its demethylated form but FMISO is not a substrate for this reaction. Additionally, ~7% (in humans) to ~14% (in mice) is conjugated to glucuronide, and small amounts (<5%) are converted to aminoimidazole. Substantial amounts of MISO are recoverable in feces. Fecal bacteria are able to reduce misonidazole only in the absence of oxygen. At treatment level dosing, the plasma half-lives of both FMISO and MISO range from 8 – 17.5 hours[28]. Parent molecule and glucuronide metabolites are primarily excreted in the urine[29,30,31].

FMISO Mouse Studies. Biodistribution studies in mice have used different transplanted tumors and compared [^{3}H]FMISO with the [^{18}F]FMISO. The only normal organs with significant uptake were those associated with nitroimidazole metabolism and excretion, i.e. liver and kidney. Mice bearing a variety of tumors of different sizes received a single injection of [^{3}H]FMISO and were sacrificed at 4 hr[32]. The results are shown in Table 4. For small KHT tumors, the tumor to blood ratios (T:B) of 2.3-2.9 were sufficiently high to allow tumor detection with imaging. Larger KHT tumors, with a reported hypoxic fraction >30%, had higher T:B ratios. RIF1 tumors in C3H mice have a hypoxic fraction of ~1.5% and had the lowest tumor:blood ratios: 1.7-1.9. This correlation between T:B ratios and hypoxic fraction was encouraging, but did not hold true across all tumor types. C3HBA mammary adenocarcinomas of the same size as the RIF1 and small KHT tumors, had hypoxic fractions of 3-12%, but had the highest T:B ratios, 4.0-4.7. Within tumor type, increasing hypoxia was associated with increased uptake of labeled FMISO, but comparisons across tumor types were more difficult, perhaps because of heterogeneity within the tumors.

Table 4. Biodistribution of [^{3}H]fluoromisonidazole in C3H mice32

Tumor	Drug dose	Tumor: Blood ratios	Tumor volumes. mm^{3*}	Estimated hypoxic fraction$^+$
KHT	5 mmol/kg	2.41	175 ± 16	7-12%
KHT	5 mmol/kg	2.29	110 ± 25	
KHT	20 mmol/kg	2.76	159 ± 39	
KHT	20 mmol/kg	2.86	123 ± 37	
KHT	5 mmol/kg	5.58	580 ± 26	>30%
KHT	5 mmol/kg	8.34	574 ± 66	
RIF1	5 mmol/kg	1.69	158 ± 23	~1.5%
RIF1	20 mmol/kg	1.76	159 ± 15	
RIF1	20 mmol/kg	1.86	136 ± 37	
C3HBA	5 mmol/kg	4.66	101 ± 13	3-12%
C3HBA	5 mmol/kg	3.96	137 ± 37	

* Tumor volumes are mean ± standard deviation for 5 tumors/group. Animals sacrificed at 4 hr.
\+ Hypoxic fractions are taken from[33] for tumors of comparable size.

In individual KHT tumors or RIF1 tumors, there was no correlation between regional flow and regional FMISO retention at 4 hr after tracer injection. The r^2-values for KHT and RIF1 tumors were 0.0 and 0.05, respectively. Regional blood flow did not correlate with FMISO retention in normal tissues that retained high levels of FMISO, specifically in liver (a principal site of nitroimidazole metabolism) and kidney (the main route of excretion) nor in tissues such as muscle and brain.

The mouse biodistribution studies described above provided useful information about relative tumor FMISO distribution at a single time post-injection and demonstrated T:B ratios adequate for PET imaging. Tumor bearing rats have also been imaged dynamically to provide biodistribution data for all tissues after sacrifice. The well-characterized 36B10 transplantable rat glioma was grown subcutaneously in Fischer rats[34] to obtain time activity data for tumors and blood up to 2 hr after FMISO injection. These studies showed that tumors steadily accumulated [^{3}H]FMISO activity that exceeded levels in blood after ~20 min.

Dogs with spontaneous osteosarcomas, a tumor that is frequently radio-resistant, have also been imaged after injection of [^{18}F]FMISO. These images allowed the investigator to draw regions of interest around tumor and normal tissue in each imaging plane. Timed blood samples were also drawn and plasma was counted in a gamma well so that, after decay correction, imaging and blood data could be converted to units of µCi/g. Blood time activity curves for dogs were similar when presented in comparable

units[32]. Time activity curves for blood, muscle and for a region from a forelimb osteosarcoma in one dog are shown in Figure 3.

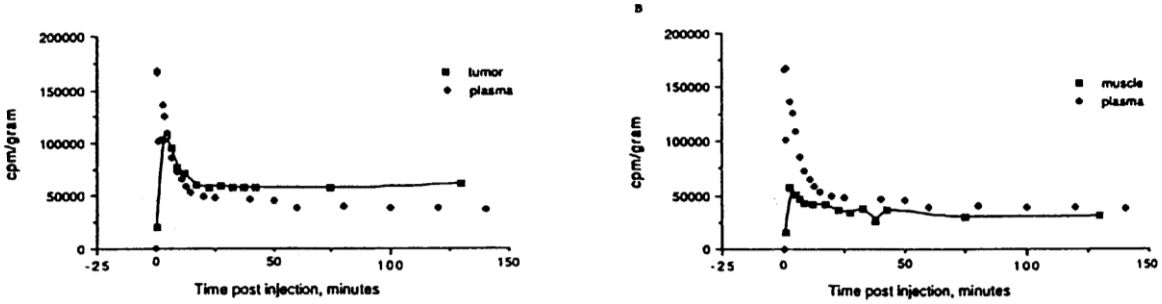

Figure 3. FMISO blood and tissue clearance curves in a dog with osteosarcoma

Muscle equilibrated with blood after 60 min, while the selected tumor region continued to accumulate FMISO above blood levels. The mean plasma half-time, calculated from five dogs, was 284±20 min for the slow component. The dog studies showed marked regional variation in FMISO uptake. These imaging studies with dogs confirmed the feasibility of imaging and suggested that multi-plane images in individual tumors would be necessary to assess regional variation in tumor hypoxia.

2. FMISO CELL TOXICITY STUDIES

Early studies evaluating the biological behavior of FMISO used several model systems with varying levels of complexity. The studies performed *in vitro* employed cells in monolayer cultures and multi-cellular spheroids. Multicellular spheroids are aggregates of cells that grow in culture and mimic small nodular tumors. Cell uptake and distribution studies in spheroids were done using [^{3}H]FMISO[35].

The *in vitro* studies of tumor cells and rodent fibroblasts measured the O_2-dependency of FMISO uptake and the time course of uptake at O_2 levels approaching anoxia. Uptake of FMISO by cells growing in monolayer cultures depended strongly on oxygen concentration, with maximum uptake under anoxic conditions and a decrease to 50% of maximum binding at levels between 700 to 2300 ppm in several different cell lines (Table 4a). The O_2-dependency of binding was a mirror image of the curve for sensitization to radiation by O_2, an advantageous characteristic for a hypoxia tracer intended to assess radiobiologically significant levels of hypoxia.

Table 5. Inhibition of [^{3}H]FMISO Binding by Oxygen *in vitro*[36]

Cell Line	O_2 concentration to inhibit binding by 50% (ppm)
RIF1	720
V79	1400
EMT6	1500
CaOs1	2300

Uptake of FMISO by multi-cellular spheroids provided visual and quantitative measures of hypoxia. Autoradiographs of 0.8 mm V79 spheroids after 4 hr incubation with [^{3}H]FMISO revealed heavily labeled cells in an intermediate zone between the well oxygenated periphery and the necrotic center. Uptake in anoxic spheroids matched that in anoxic monolayer cultures; oxygenated spheroids did not accumulate tracer, and hypoxic spheroids had intermediate uptake.

Whitmore et al. performed preliminary toxicity studies on MISO using Chinese hamster ovary cells [37]. Uncharacterized toxic products suspected of being either nitroso or hydroxylamine derivatives formed only under hypoxic conditions and were capable of sensitizing both hypoxic and aerobic cells to the damaging effects of radiation. These products have been further characterized by Flockhart and are differently distributed depending upon the species. In humans the demethylated molecule never exceeds 10% of the total MISO, and the amine never exceeds 2% in extracellular fluid[31]. The demethylation reaction is not possible with FMISO, which lacks a methoxy substituent.

3. ANIMAL TOXICITY STUDIES: MISO and FMISO

The literature provides a few animal studies of the toxicity of nitroimidazoles. The octanol/water partition coefficients for MISO and FMISO are 0.43 and 0.41, respectively; the LD50's in adult male Balb/C mice for MISO and FMISO are 1.8 mg/g (1.3-2.6) and 0.9 mg/g, respectively[38]. The serum half-lives of orally administered MISO and FMISO in mice were 2.3 hrs (range 1.87-2.92) and 2.0 hrs (range 1.79-2.24), respectively. A subsequent study of LD50's in 21 to 32 g, nine-month old, female C3H/HeJ mice gave toxicities of 0.62 to 0.64 mg/g for FMISO[39]. The long component of the plasma half-life of FMISO in humans is similar to MISO (8-17 hrs). FMISO is cleared primarily through the kidneys. Its volume of distribution is large, approximating that of total body water. Favorable tumor-to-normal tissue ratios for imaging are obtained at low doses of administered drug. These ratios were obtained in 15 kg dogs with a dose of 1 mg/kg.

After oral dosing exceeding a schedule-dependent cumulative threshold, misonidazole induces a peripheral neuropathy in humans, although such dosing far exceeds the PET imaging dose requirements. Because FMISO will be administered intravenously, the neurotoxicity of intravenous administration was evaluated in rats using a battery of routine clinical, neurofunctional, biochemical, and histopathologic screening methods[40]. Male Sprague-Dawley rats were administered intravenous doses of misonidazole at 0

(vehicle control), 100, 200, 300, or 400 mg/kg daily for 5 days per week for 2 weeks. Animals were evaluated for functional and pathological changes following termination of treatment and at the end of 4 weeks. During the dosing phase, hypoactivity, salivation, rhinorrhea, chromodacryorrhea, rough pelage and ataxia were observed at 400 mg/kg and body weight gain of the 300 and 400 mg/kg groups was significantly decreased relative to the vehicle controls (24% and 49% respectively) and related to reductions in food consumption of 8% and 23%. Although most 400 mg/kg animals appeared normal immediately after the dosing regimen, rotorod testing precipitated a number of clinical signs including: ataxia, impaired righting reflex, excessive rearing, tremors, vocalization, circling, head jerking, excessive sniffing and hyperactivity. All animals recovered and appeared normal through study termination. There were no treatment-related effects on motor activity, acoustic startle response, rotorod performance, forelimb group strength, toe and tail pinch reflexes, tibial nerve beta-glucuronidase activity or tail nerve conduction velocity. No microscopic changes were detected in peripheral nerves. Necrosis and gliosis were seen in the cerebellum and medulla of the 400 mg/kg animals after treatment and gliosis in these same brain regions was observed in the 300 and 400 mg/kg groups at a month after dosing. These results show that intravenous administration of misonidazole to rats causes dose-limiting central nervous system toxicity without effects on peripheral nervous tissue.

4. HUMAN TOXICITY STUDIES: MISO

Human studies of nitroimidazoles date back to the 1970's when several nitroimidazole derivatives were tested as oxygen mimetics in clinical research trials involving tumors that were presumed to be hypoxic. The goal was to sensitize them to cytotoxic levels of photon radiation so that they retained the beneficial 3-fold enhancement ratio characteristic of normoxic tissues[41,42,43]. Our knowledge of the toxic effects of 2-nitroimidazoles in humans is based principally on misonidazole, a close analog of fluoromisonidazole (Figure 1), and studies that used doses that were considered effective to enhance the cytotoxicity of radiotherapy. These human studies, no longer in progress, have been reviewed[44]. There have been no reported harmful effects until cumulative doses exceeded a few grams, which is vastly larger than the dosing required for PET imaging.

Gray reported preliminary human pharmacokinetic measurements using six healthy volunteers[45]. Subjects received single oral doses ranging from 1 g to 4 g. The peak serum level at 2 hours was 65 µg/mL and the drug serum half-life was 13.1 ± 4.0 hrs. A linear relationship was demonstrated between administered dose and serum level. Based on animal studies, a serum level of 100 µg/mL was considered necessary for effective radiosensitization and the oral dose calculated to achieve that serum level was 6.5 g. Single oral doses of 4-10 g were administered to 8 patients with advanced cancer and a life expectancy limited to 12 months. All patients experienced some degree of nausea, vomiting and anorexia for 24 hours. One of the eight had insomnia. At 10 g the nausea and vomiting were extreme, and the anorexia lasted for a week. Peak serum

levels were obtained between 1 and 3 hrs. The serum half-life ranged from 9-17 hrs with the median at 14 hrs.

Clinical studies employing multiple dosing of MISO have also been reported and peripheral neuropathy (PN) was the manifestation of toxicity that became dose limiting with daily doses of 3-5 g/m2. The results of a sequential dose reduction study46 are shown in Table 6:

Table 6. Clinical toxicity of misonidazole

Dose (g/m^2)	Doses/wk.	Weeks	Affected Patients	Total Patients	% Pts. with peripheral neuropathy
3-5	5	3	12	16	75
2	2	3	2	6	33
0.4-0.8	3-5	3-6	1	6	16

This data demonstrates the dose proportionality of the drug's primary toxicity during chronic administration at doses that far exceed those used in PET imaging. Limiting the total dose and giving no more than two doses in one week minimized toxicity.

Significantly lower peripheral neuropathic (PN) toxicity for therapeutic doses has been observed with weekly dosing schedules: 1 of 12 with PN at 1-2 g/m^2 for 6 weeks[47] and 0 of 10 at 3 g/m^2 for 4 weeks[48]. This is presumably due to the fact that the drug, which has a long serum half-life, is allowed to clear completely from the body. Dische had a similar experience, noting that calculations by surface area produce the most consistent correlation of oral dose to plasma level and that the maximum recommended safe dose was 12 g/m^2 over no less than 18 days[49]. Neuropathies were generally, but not always, reversible when the drug was discontinued.

There have been two fatalities attributed to the drug[50]. Both patients had advanced malignant disease and died in convulsions: One patient received 51 g in 6 fractions over 17 days, and the other patient received 16 g in 2 doses over 3 days.

The above data supports the conclusion that FMISO's primary toxicity is likely to be peripheral neuropathy, which is dependent upon frequency and dose level. There is no evidence to suggest that FMISO poses a risk for PN when administered as an imaging agent for PET as described herein. The risk for PN in fact appears to be minimized or absent even at therapeutic doses that far exceed those necessary for PET imaging.

5. [^{19}F]FMISO HUMAN TOXICITY

A search for articles dealing with the human toxicity of fluoromisonidazole (FMISO) yields no results. Therefore this assessment relies on animal studies and similarities among related chemical entities. The octanol/water partition coefficients for MISO and

FMISO are 0.43 and 0.41, respectively; the LD50's in adult male Balb/C mice for MISO and FMISO are 1.8 mg/g (1.3-2.6) and 0.9 mg/g, respectively[38] and in CH3 mice the LD50 is 0.6 mg/g for FMISO[39]. Using the relative toxicity factors from Paget (1965)[51] of 1.0 for mice and 9.8 for humans, the projected LD_{50} values are:

LD_{50} values	Misonidazole	Fluoromisonidazole
Concentration for human	0.184 g/kg	0.06-0.09 g/kg
Dose for 70 kg subject	12.86 g	6.43 g

The MISO values by this calculation are conservative when compared with the findings in early human trials (see Section 7, MISO Human Safety Studies). The serum half-lives of orally administered MISO and FMISO in mice were 2.3 hrs (range 1.87-2.92) and 2.0 hrs (range 1.79-2.24), respectively. The long component of the plasma half-life of FMISO in humans is similar to MISO (8-17 hrs). FMISO is cleared primarily through the kidneys.

The maximum dose to humans reported in imaging protocols was 1 mg/kg or 70 mg for a 70 kg subject; no adverse events have been reported. These studies are reported in Part VII. This is about 0.1% of the projected LD_{50}. Total patient imaging doses of the current radiopharmaceutical formulation contain ≤ 15 µg of fluoromisonidazole and less than 35 µg of other nitroimidazole derivatives. This is <0.001% of the projected LD50. The drug has had no toxic effects at these doses based upon a review of 5400 patients included in MISO studies[44] and over 269 patients studied with tracer doses of [^{18}F]FMISO, as summarized in this document (Section 9).

6. [^{18}F]FMISO HUMAN TOXICITY

Since the half-life of fluorine-18 is only 110 minutes, toxicity studies are not possible with the radiolabeled agent. The misonidazole data presented and the [^{19}F]FMISO calculations presented above in sections 4 and 5 should be the basis for both animal and human toxicity characterization and conclusions. The radiation dose associated with [^{18}F]FMISO is discussed separated in Part VI.

7. MISO HUMAN SAFETY STUDIES

Misonidazole for Therapy. In addition to their role as imaging agents, nitroimidazoles have been studied as therapeutic radiosensitizers (oxygen mimetics). These studies of over 7000 patients in 50 randomized trials have been reviewed[44]. Oral MISO was the agent in 40 of the trials involving about 5400 patients. The maximum doses used were 4 g/m^2 in a single dose and 12 g/m^2 as a total dose. The most common serious/dose limiting side effect was peripheral neuropathy with a latency period of several weeks.

The neuropathy was prolonged and, in some cases, irreversible. Nausea, vomiting, skin rashes, ototoxicity, flushing and malaise have also been reported at therapeutic dosing levels that vastly exceed imaging dose requirements. While these molecules are no longer used as clinical radiosensitizers, the results show the range of human experience with nitroimidazoles, and, in particular, support a reliable trend towards safety at imaging range dosing.

A 1978 study of oral misonidazole (MISO) as a radiosensitizing agent in human astrocytoma found good absorption, peak plasma levels between 1 and 4 hours and a half-life between 4.3 and 12.5 hours. Doses limited to 12 g/m^2 produced some nausea and vomiting but no serious side effects[48]. In an earlier study, Gray found a wide variation in tumor/plasma distribution ratios in six cases of advanced human metastatic breast cancers and soft tissue sarcomas[45]. The maximum dose in this study was 10 g, which caused a week of anorexia. Patients receiving up to 140 mg/kg tolerated the drug well.

8. [^{19}F]FMISO HUMAN SAFETY STUDIES

We are unaware of, nor did a literature search show, any human studies of [^{19}F]FMISO safety in humans beyond the carrier [^{19}F]-FMISO associated with the [^{18}F]FMISO human studies described below.

9. [^{18}F]FMISO HUMAN SAFETY STUDIES

[^{18}F]FMISO is a radiolabeled imaging agent that has been used for investigating tumor hypoxia with PET. It is composed of ≤ 15 µg of fluoromisonidazole labeled with ≤ 10 mCi of radioactive ^{18}F at a specific activity >1 Ci/mg at the time of injection. The drug is the only active ingredient and it is formulated in ≤ 10 mL of 5% ethanol in saline for intravenous injection. The radiochemical purity of the [^{18}F]FMISO is >95%. Hypoxia imaging in cancer was reviewed in several recent publications[22,52,53,54]. [^{18}F]FMISO is a robust radiopharmaceutical useful in obtaining images to quantify hypoxia using PET imaging[55,56,57]. It is the most commonly used agent for PET imaging of tissue/tumor hypoxia[58,52,53,54,59,60,61].

Positron emission scanning with ^{18}F-FMISO has been studied over the past ten years in Australia, Switzerland, Denmark, Germany, China and in the United States under RDRC approval or its equivalent. Several published studies from the United States are from the University of Washington in Seattle. Since 1994 up to 4 injections of FMISO, each followed by a PET scan, have been performed in Seattle alone on approximately 300 patients; data have been published on over 133 of these. [^{18}F]FMISO has been used to image ischemic stroke, myocardial ischemia and a wide variety of malignancies. Although the papers listed in Table 8 total nearly 700 patients, we have taken a conservative approach in the text to reduce possible duplication. Nonetheless as many as 4 ^{18}F-FMISO injections and PET scans have been performed in over 600 different

patients represented in the published papers as listed in Part VII, Previous Human Experience. Administered doses ranged from approximately 3 to 30 mCi (100-1100 MBq). As would be expected based upon the above safety assessment of the agent when dosed and used for imaging, no adverse events have been attributed to ^{18}F-FMISO in any of these reports. One patient with advanced nasopharyngeal cancer experienced a Grade 3 febrile neutropenia and a Grade 1 mucositis and stomatitis that were definitely related to multiple chemotherapy agents and unrelated to FMISO.

10. FMISO GENOTOXICITY AND MUTAGENICITY

Multiple studies have found genetic transformations due to misonidazole and related nitroimidazoles using in vitro assays. The murine C3H/10T½ cell line (mouse embryo fibroblast) has a normal spontaneous transformation frequency of $<10^{-5}$ but these cells undergo oncogenic transformation in vitro when exposed to chemical and physical agents. The frequency of transformants with 3 days exposure to 1 mM drug was 2.27± 0.38 x 10^{-4} for FMISO and 4.55 ± 0.95 x 10^{-4} for misonidazole[62]. Although these values are about three to five times the background rate, this level of drug exposure would require about 10 grams of drug in a human. Imaging studies will inject ≤ 15 µg, or about 0.00015%.

FMISO and MISO were mutagenic when assayed by the AMES protocol using specific Salmonella typhimurium strains. MISO showed an increasing growth of revertants from 0 at 1 µg drug per plate to ~1500 at 100 µg per plate and ~6,000 at 1,000 µg per plate containing 0.1 mL of tester strain bacteria; FMISO showed fewer revertants , ~1,000 at 100 µg drug per plate and only ~600 revertants at 10 µg per plate[63]. In other cell lines, the frequency of unscheduled DNA synthesis was used as an index of genotoxicity. In this assay, [^{3}H]-thymidine incorporation in units of dpm/µg of DNA is used to quantify DNA synthesis. For a 1 mM dose of FMISO, the rate was 54 ± 6 for hepatocytes, 187 ± 14 for BL8 (nontransformed) cells and 217 ± 11 for JB1 (transformed) cells[64], with very similar values for MISO). For comparison, the control rate of DNA synthesis was 54 ± 4, 179 ± 15 and 158 ± 14, respectively for the three cell lines. This work concluded that in hypoxic cells nitroimidazoles react much more with thiols than with DNA. While each of these three tests detected low level alterations to DNA, exposure was both several orders of magnitude greater than, and of longer duration than that required in PET imaging with [^{18}F]FMISO. Drug exposure for imaging studies is below the levels where any genotoxicity was observed.

11. ADVERSE EVENTS AND MONITORING FOR TOXICITY

No adverse events have been attributed to PET imaging/diagnostic administration of [^{18}F] FMISO at the levels described herein in well over 1,000 injections, based upon up to 4 injections administered to each of over 600 patients. Thus no adverse effects are expected as a result of the IV administration of [^{18}F]FMISO for typical PET imaging

applications such as tumor hypoxia. The proposed [^{18}F]FMISO imaging dose is less than 0.001% of the recommended safe intravenous dose.

For purposes of informed consent regarding reasonably foreseeable risks to subjects in trials utilizing [^{18}F]FMISO, the following potential adverse effects are considered extremely rare:

- Risks related to allergic reaction that may be life threatening
- Injection related risks that may include infection, or extravasation of the dose that may lead to discomfort, localized pain, temporary loss of local function, and self limited tissue damage,

These risks are minimized by the requirement that appropriately trained and licensed/certified personnel prepare, deliver and administer the agent. The subject should be monitored per institutional standards for PET imaging studies. Emergency equipment, procedures, and personnel should be in place per institutional standards for imaging performed with intravenous contrast.

Radiation from ^{18}F carries an associated risk to the patient. The organ and total body doses associated with FMISO PET imaging are comparable to or lower than those associated with other widely used clinical nuclear medicine procedures and are well below the maximum individual dose suggested for investigational radiopharmaceuticals by the FDA.

12. SAFETY AND TOXICITY OF THE OTHER COMPONENTS OF THE FINAL [^{18}F]FMISO DRUG PRODUCT

The [^{18}F]FMISO is purified by HPLC using an eluent of 5% ethanol, USP. The injected does is in up to 10 mL of 5% ethanol, or a maximum of 0.5 mL of ethanol. This is less than 5% of the amount of ethanol in one beer. In Registry of Toxic Effects of Chemical Substances (RTECS) the LD_{Lo} is given as 1.4 g/kg orally for producing sleep, headache, nausea and vomiting. Ethanol has also been administered intravenously to women experiencing premature labor (8 g/kg) without producing any lasting side effects[65] (Jung 1980). Based upon these reports and experience with hundreds of patients over the past decade receiving this amount of ethanol in injectates, ethanol should not pose any danger of toxicity in this study.

The other components of the final product solution are USP grade sterile water for injection and sterile saline. These are all nontoxic for USP grade injectables at the concentrations used. The final product is at pH 7 and the final injection volume is ≤10 mL.

The potential contaminants in the final [^{18}F]FMISO drug product are: acetone, acetonitrile, Kryptofix® [2.2.2], other reaction products. Residual solvents in the final

product are limited to 5,000 ppm (µg/mL) of acetone and 400 ppm of acetonitrile. Acetone is used to clean the TRACERLab FX_{F-N} system. Acetonitrile is used to dissolve the Kryptofix® [2.2.2] and is the solvent for the reaction. The permissible level of acetonitrile in the final product is ≤400 ppm, the USP permissible level of acetonitrile in 2-[^{18}F]FDG. The allowable level for acetone is <5,000 ppm. Acetone is a Class three solvent. This class of solvents includes no solvent known as a human health hazard at levels normally accepted in pharmaceuticals. Therefore this limit is based upon the FDA's Guidance for Industry ICH Q3C-Tables and List (November 2003 Revision 1), page 7, where it considers 5,000 ppm in 10 mL, 50 mg or less per day, of Class 3 residual solvents as an acceptable limit without additional justification.

The toxicity for Kryptofix® [2.2.2] has not been reported (RTECS Number Kryptofix® [2.2.2] MP4750000) although this reagent has been investigated as a therapeutic in mice for chelation therapy after strontium exposure. The FDA has proposed a maximum permissible level of 50µg/mL of Kryptofix® [2.2.2] in 2-[^{18}F]FDG, therefore this maximum permissible level will also apply to the [^{18}F]FMISO final product.

There are trace amounts of other reaction products in the final product. The principal trace impurity is 1-(2,3-dihydroxy)propyl-2-nitroimidazole but other impurities are possible. For this reason the upper limit is set at 35 µg for the total of other materials in the final injectate that are retained more than 3 minutes on C18 HPLC (Aquasil 2X150 mm at 0.3 mL/min) and have UV absorbance at 254, 280 or 327 nm. The 35 µg is determined by assuming that the UV absorbing compounds have the same molar extinction coefficient as FMISO.

VI. BIODISTRIBUTION AND RADIATION DOSIMETRY OF FMISO

^{18}F is a positron emitter with a half-life of 110 minutes. Intravenously injected [^{18}F]-FMISO distributes throughout the total body water space, crossing cell membranes, including the blood-brain-barrier, by passive diffusion. [^{18}F]FMISO is bound and retained within viable hypoxic cells in an inverse relationship to the O_2 concentration. The uptake of [^{18}F]FMISO in normal human tissues has been measured and used to estimate the radiation absorbed dose associated with the imaging procedure. Dosimetry studies were performed at the University of Washington and have been published in the peer-reviewed Journal of Nuclear Medicine[55].

Sixty men and women were subjects in the study,. Of these, 54 had cancer, three had a history of myocardial ischemia, two were paraplegic and one had rheumatoid arthritis. After injecting 3.7 MBq/kg (0.1 mCi/kg), urine and normal tissues distant from each subject's primary pathology were imaged repeatedly to develop time-activity curves for target tissues. All tissues demonstrated a rapid uptake phase and first-order near-logarithmic clearance curves. All tissues receive a similar radiation dose, reflecting the similarity of biodistribution to that of water. Total tissue uptake data were normalized

for a 1.0 MBq injection into a 70 kg man. The organ curves are shown in Figure 4 and Figure 5[55]:

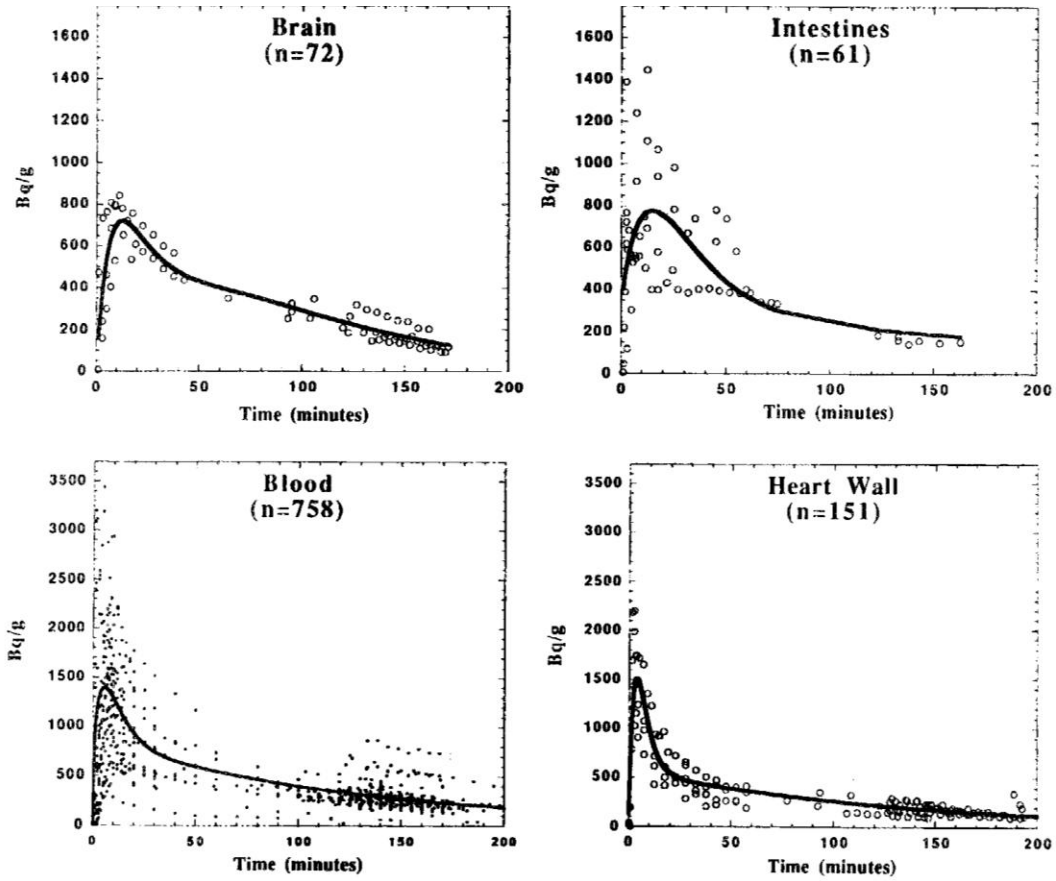

Figure 4. Activity of FMISO in 4 source organs with best fit used to determine AUC. The data are normalized to 1 MBq/70 kg bw.

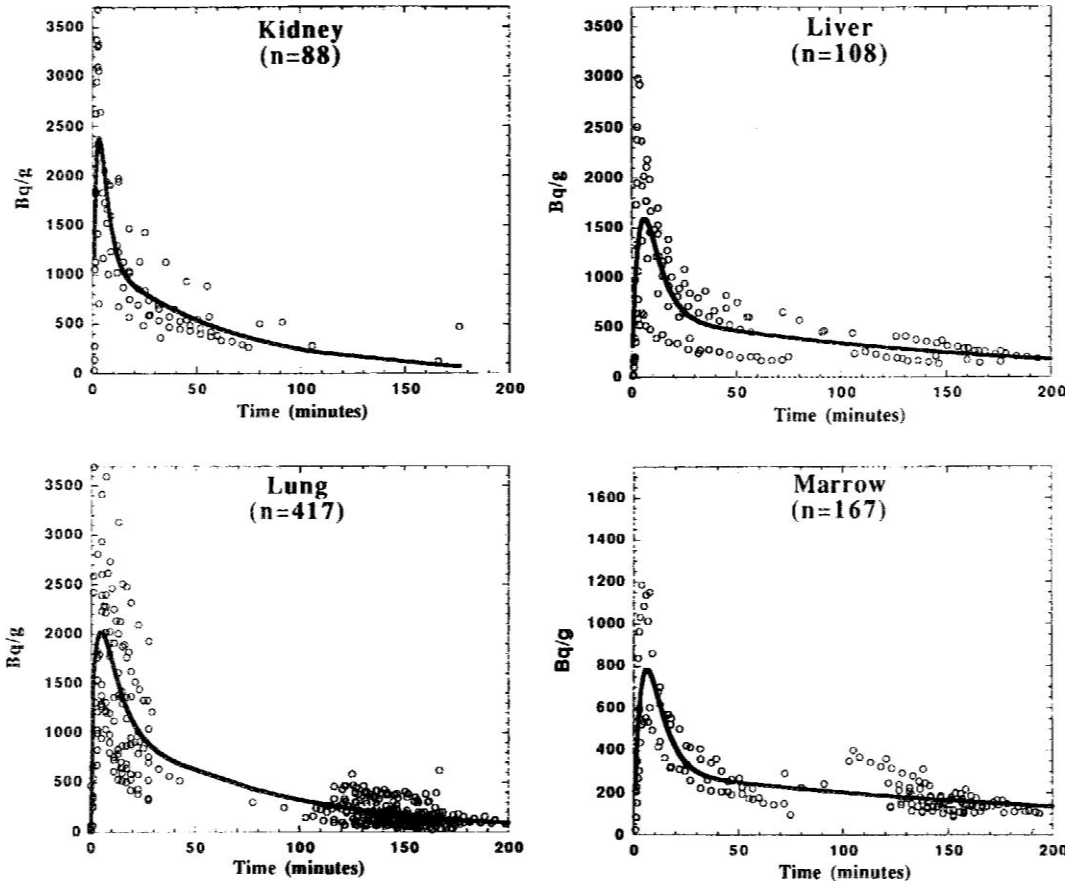

Figure 5. Activity of FMISO in four other source organs with best fit used to determine AUC. The data are normalized to 1 MBq/70 kg bw.

Radiation dose to the bladder wall varied with voiding interval from 0.021-0.029 mGy/MBq. *Figure **6***[55] is a composite of the integrated ^{18}F urine activity of 42 samples from 20 studies. The line is the best fit to the data and was used to determine AUC for individual patients. Note that the mean total excretion is about 30 kBq, or 3% of the injected dose.

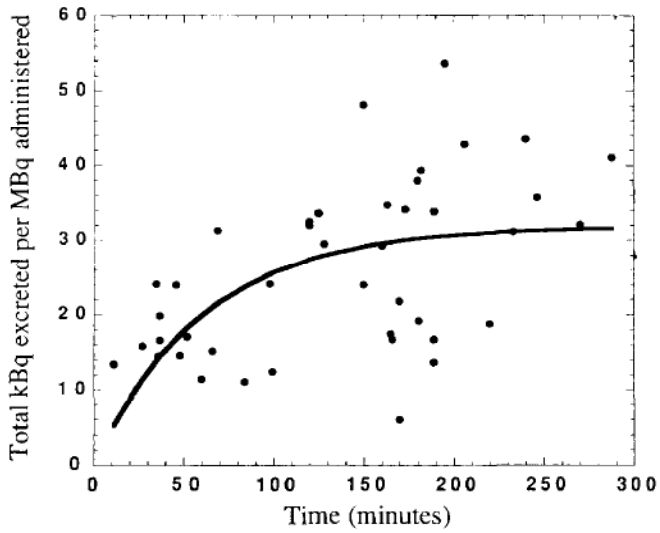

Figure 6. Bladder activity
from injection of 1 MBq of [^{18}F]FMISO/ 70 kg bw.

From these human data, radiation absorbed doses to organs was calculated using the MIRD schema and the results are shown in Table 7[55].

Table 7. Radiation Absorbed Dose to Organs

Tissue	Mean (mGy/MBq)	Mean (mrad/mCi)	Total / 7 mCi (mrad)
adrenals	0.0166	61.4	430
brain	0.0086	31.8	223
breasts	0.0123	45.5	319
gall bladder wall	0.0148	54.8	383
lower large intestine	0.0143	52.9	370
small intestine	0.0132	48.8	342
stomach	0.0126	46.6	326
upper large intestine	0.0140	51.8	363
heart wall	0.0185	68.5	479
kidneys	0.0157	58.1	407
liver	0.0183	67.7	474
lungs	0.0099	36.6	256
muscle	0.0142	52.5	368
ovaries	0.0176	65.1	456
pancreas	0.0179	66.2	464
red marrow	0.0109	40.3	282
bone surface	0.0077	28.5	199
skin	0.0048	17.8	124
spleen	0.0163	60.3	422
testes	0.0146	54.0	378
thymus	0.0155	57.4	401
thyroid	0.0151	55.9	391
urinary bladder wall	0.0210	77.7	544
uterus	0.0183	67.7	474
eye lens	0.0154	57.0	399
Total body	0.0126	46.6	325

Calculated total body dose for a 70 kg man injected with 3.7 MBq/kg was 0.013 mGy/MBq; for a 57 Kg woman it was 0.016 mGy/MBq. Effective dose equivalents were 0.013 mSv/MBq for men and 0.014 mSv/MBq for women. Ninety-seven percent of the injected radiation was homogenously distributed in the body, leaving only 3% for urinary excretion. Doses to smaller organs not directly determined by visualization, such as the lens, were calculated assuming average total-body concentrations. The absence of tracer visualized in images of those organs indicated that accumulation there was not increased.

The radiation exposure from [^{18}F]FMISO is equal to or lower than that of other widely used nuclear medicine studies. Increasing the frequency of voiding can reduce radiation dose to the normal organ receiving the highest radiation absorbed dose, the bladder

wall. Potential radiation risks associated with a typical PET study utilizing this agent are within generally accepted limits.

VII. [^{18}F]FMISO PREVIOUS HUMAN EXPERIENCE AND ASSESSMENT OF CLINICAL POTENTIAL

[^{18}F]FMISO is a radiolabeled imaging agent that has been used for investigating tumor hypoxia with PET. A hypoxia-imaging agent should be independent of blood flow, which is achieved when the partition coefficient of the tracer is close to unity and imaging is done at a time when the tracer distribution has equilibrated with its entry into the cells. [^{18}F]FMISO is an azomycin-based hypoxic cell sensitizer that has a nearly ideal partition coefficient and binds covalently to molecules at rates that are inversely proportional to intracellular O_2 concentration, rather than by some downstream biochemistry. It is composed of ≤ 15 µg of fluoromisonidazole labeled with ≤ 10 mCi of radioactive ^{18}F at a specific activity ≥1 Ci/mg at the time of injection. The drug is the only active ingredient and it is formulated in ≤ 10 mL of 5% ethanol in saline for intravenous injection. The radiochemical purity of the [^{18}F]FMISO is >95%.

Hypoxia imaging in cancer was reviewed in several recent publications[22,52,53,54]. [^{18}F]FMISO is a robust radiopharmaceutical useful in obtaining images to quantify hypoxia using PET imaging[55,56,57]. It is the most commonly used agent for PET imaging of hypoxia [58,52,53,54,59,60,61]. While its biodistribution properties do not result in high contrast images, they result in images at 2 hours after injection that unambiguously reflect regional partial pressure of oxygen, Po_2, and hypoxia in the time interval after the radiopharmaceutical was administered.

Positron emission scanning with [^{18}F]FMISO has been studied over the past ten years in Australia, Switzerland, Denmark, Germany and in the United States under RDRC approval or its equivalent. Several published studies from the United States are from the University of Washington in Seattle. Since 1994, approximately 300 patients have undergone FMISO PET scans in Seattle, at least 133 of whom are included in Table 8 of published studies. [^{18}F]FMISO has been used to image ischemic stroke, myocardial ischemia and a wide variety of malignancies.

Although published papers, as listed in Table 8, total 694 patients, we have elected to remain conservative in that duplication of some patients is possible. Nonetheless we are confident that over 600 unique patients have undergone up to 4 injections of the agent as described herein. The most recent papers, summarized briefly below, conservatively appear to represent at least 66 unique and recent patients, for example. Administered doses ranged from approximately 3 to 30 mCi (100 - 1100 MBq). No adverse events were noted in any of these papers, which are summarized in Table 8.

There have been several recent papers published on FMISO use as a PET imaging agent in humans. Representative papers from key groups in ongoing [F-18]FMISO PET imaging are summarized below.

In a paper published in 2009, Swanson[67] reported on 24 patients with glioblastoma who underwent T1Gd, T2, and 18F-FMISO studies either prior to surgical resection or biopsy, after surgery but prior to radiation therapy, or after radiation therapy. Abnormal regions seen on the MRI scan were segmented, including the necrotic center (T0), the region of abnormal blood-brain barrier associated with disrupted vasculature (T1Gd), and infiltrating tumor cells and edema (T2). The 18F-FMISO images were scaled to the blood 18F-FMISO activity to create tumor-to-blood ratio (T/B) images. The hypoxic volume (HV) was defined as the region with T/Bs greater than 1.2, and the maximum T/B (T/Bmax) was determined by the voxel with the greatest T/B value. They found that the HV generally occupied a region straddling the outer edge of the T1Gd abnormality and into the T2. A significant correlation between HV and the volume of the T1Gd abnormality that relied on the existence of a large outlier was observed. There was consistent correlation between surface areas of all MRI-defined regions and the surface area of the HV. The T/Bmax, typically located within the T1Gd region, was independent of the MRI-defined tumor size. Univariate survival analysis found the most significant predictors of survival to be HV, surface area of HV, surface area of T1Gd, and T/Bmax. They concluded that hypoxia may drive the peripheral growth of glioblastomas[67].

In a 2008 paper by Lin, seven patients with head and neck cancers were imaged twice with FMISO PET, separated by 3 days, before radiotherapy. Intensity-modulated radiotherapy plans were designed, on the basis of the first FMISO scan, to deliver a boost dose of 14 Gy to the hypoxic volume, in addition to the 70-Gy prescription dose. The same plans were then applied to hypoxic volumes from the second FMISO scan, and the efficacy of dose painting evaluated by assessing coverage of the hypoxic volumes using Dmax, Dmin, Dmean, D95, and equivalent uniform dose (EUD). The authors found similar hypoxic volumes in the serial scans for 3 patients but dissimilar ones for the other 4. There was reduced coverage of hypoxic volumes of the second FMISO scan relative to that of the first scan. The decrease was dependent on the similarity of the hypoxic volumes of the two scans. They concluded that the changes in spatial distribution of tumor hypoxia, as detected in serial FMISO PET imaging, compromised the coverage of hypoxic tumor volumes achievable by dose-painting IMRT. However, dose painting always increased the EUD of the hypoxic volumes[70].

In a study published in 2008, Roels et. al. investigated the use of PET/CT with fluorodeoxyglucose (FDG), fluorothymidine (FLT) and fluoromisonidazole (FMISO) for radiotherapy (RT) target definition and evolution in rectal cancer. PET/CT was performed before and during preoperative chemoradiotherapy (CRT) in 15 patients with resectable rectal cancer. They concluded that FDG, FLT and FMISO-PET reflect different functional characteristics that change during CRT in rectal cancer. FLT and FDG show good spatial correspondence, while FMISO seems less reliable due to the non-specific FMISO uptake in normoxic tissue and tracer diffusion through the bowel wall. FDG and FLT-PET/CT imaging seem most appropriate to integrate in preoperative RT for rectal cancer[75].

Nehmeh et. al. reported a study on 20 head and neck cancer patients in a 2008 paper. Of these, 6 were excluded from the analysis for technical reasons. All patients underwent an FDG study, followed by two (18)F-FMISO studies 3 days apart. The authors found that variability in spatial uptake can occur between repeat (18)F-FMISO PET scans in patients with head and neck cancer. Of 13 patients analyzed, 6 had well-correlated intratumor distributions of (18)F-FMISO-suggestive of chronic hypoxia. They concluded that more work is required to identify the underlying causes of changes in intratumor distribution before single-time-point (18)F-FMISO PET images can be used as the basis of hypoxia-targeting intensity-modulated radiotherapy[74].

In a 2008 paper Lee reported on a study that examined the feasibility of ((18)F-FMISO PET/CT)-guided IMRT with the goal of maximally escalating the dose to radioresistant hypoxic zones in a cohort of head and neck cancer (HNC) patients. (18)F-FMISO was administered intravenously for PET imaging. The CT simulation, fluorodeoxyglucose PET/CT, and (18)F-FMISO PET/CT scans were co-registered using the same immobilization methods. The tumor boundaries were defined by clinical examination and available imaging studies, including fluorodeoxyglucose PET/CT. Regions of elevated (18)F-FMISO uptake within the fluorodeoxyglucose PET/CT GTV were targeted for an IMRT boost. Additional targets and/or normal structures were contoured or transferred to treatment planning to generate (18)F-FMISO PET/CT-guided IMRT plans. The authors found that the heterogeneous distribution of (18)F-FMISO within the GTV demonstrated variable levels of hypoxia within the tumor. Plans directed at performing (18)F-FMISO PET/CT-guided IMRT for 10 HNC patients achieved 84 Gy to the GTV(h) and 70 Gy to the GTV, without exceeding the normal tissue tolerance. An attempt to deliver 105 Gy to the GTV(h) for 2 patients was successful in 1, with normal tissue sparing. The conclusion was that it was feasible to dose escalate the GTV(h) to 84 Gy in all 10 patients and in 1 patient to 105 Gy without exceeding the normal tissue tolerance. This information has provided important data for subsequent hypoxia-guided IMRT trials with the goal of further improving locoregional control in HNC patients[68].

Thorwarth et. al. published a 2008 paper on a dose painting strategy to overcome hypoxia-induced radiation resistance. 15 HNC patients were examined with 18F-FDG and dynamic 18F-FMISO PET before the start of a 70Gy radiotherapy. After approx. 20 Gy, a second dynamic 18F-FMISO scan was performed. The voxel based 18F-FMISO PET data were analyzed with a kinetic model, which allows for the determination of local tumor parameters for hypoxia and tissue perfusion. Their statistical analysis showed that only a combination of these two parameters predicted treatment outcome. They concluded that a translation of the imaging data into a reliable dose prescription can only be reached via a TCP model that includes these functional parameters. A model was calibrated using the outcome data of the 15 HNC patients. This model mapping of locally varying dose escalation factors to be used for radiotherapy planning. A planning study showed that hypoxia dose painting is feasible without a higher burden for the organs at risk[71].

Table 8. Published manuscripts reporting ^{18}F-FMISO human imaging studies

Year	Clinical Condition	n	mCi injected	MBq injected	Reference
2009	Brain Cancer	11	(7 mCi) 0.1 mCi/kg	260 (3.7 mCi/kg)	Szeto[66] (USA 2009)
2009	Brain Cancer	24	(7 mCi) 0.1 mCi/kg	260 (3.7 mCi/kg)	Swanson[67] (USA 2009)
2009	Head & Neck Cancer	28	10	370	Lee[68] (USA 2009)
2008	Brain Cancer	22	(7 mCi) 0.1 mCi/kg	260 (3.7 mCi/kg)	Spence[69] (USA 2008)
2008	Head & Neck Cancer	7	10	370	Lin[70] (USA 2008)
2008	Head & Neck Cancer	15	Not Reported	Not Reported	Thorwarth[71] (Germany 2008)
2008	Head & Neck Cancer	28	9.3-11	344-407	Lee[72] (USA, 2008)
2008	Head & Neck Cancer	3	10.8	~ 400	Thorwarth[73] (Germany, 2008)
2008	Head & Neck Cancer	20	9.3-11	344-407	Nehmeh[74] (USA, 2008)
2008	Rectal Cancer	10	8.9-11	330-398	Roels[75] (Belgium 2008)
2007	Advanced Head & Neck Cancer	14	9.4-12.2	350-450	Eschmann[76] (Germany 2007)
2007	Advanced Non-small cell lung cancer	4	7	259	Spence[77] (USA, 2007)
2007	Head & Neck Cancer	38	9.6	356	Gagel[78] (2007, Germany)
2007	Head & Neck Cancer	13	10.8	400	Thorwarth[79] (Germany, 2007)
2006	Head & Neck	24	9.7 ± 0.7	360 ± 25	Zimny[80] (Germany, 2006)
2006	Non-small cell lung cancer	21	10	370	Cherk[81] (Australia, 2006)
2006	Head and Neck Cancer	45	Not Reported	Not Reported	Rischin[82] (Australia, 2006)
2006	Head and Neck Cancer	73	10	Max 370 nom 260	Rajendran[83] (USA, 2006)
2006	Non-small cell lung cancer	8	8.9 ± 0.10	329 ± 36	Gagel[84] (Germany, 2006)

Year	Clinical Condition	n	mCi injected	MBq injected	Reference
2006	Glioma	17	0.5	18.5/kg nom 130	Cher[85] (Australia, 2006)
2005	Head & neck cancer	26	9.4-12.2	350-450	Eschmann[60] (Germany, 2005)
	Non-small cell lung cancer	14			
2004	Various brain tumors	11	3.3-11.4	123-421 Avg.= 291	Bruehlmeier [86] (Switzerland, 2004)
2004	Various cancers	49	0.1 mCi/kg	3.7/Kg nom 260	Rajendran[54] (USA, 2004)
2004	Head & neck cancer	16	7.9-0.9	292 ± 35	Gagel[87] (Germany, 2004)
2003	Ischemic Stroke	19	Not Reported	nom 130	Markus[88] (Australia, 2003)
2003	Soft tissue tumors	13	5.9-11.3	218-418 Avg.= 400	Bentzen[89] (Denmark, 2003)
2003	Soft tissue sarcoma	29	Not Reported	3.7/Kg nom 260	Rajendran[90] (USA, 2003)
2001	Brain tumors	13	Not Reported	Not Reported	Scott[91] (Australia, 2001)
2000	Ischemic Stroke	24	Not Reported	nom 130	Read[92] (Australia, 2000)
1996	Various cancers	37	Not Reported	3.7/Kg nom 260	Rasey[93] (USA, 1996)
1995	Non-small cell lung cancer	7	Not Reported	3.7/Kg nom 260	Koh[53] (USA, 1995)
1992	Various cancers	8	20-29.7	740-1100 (multiple studies)	Koh[94] (USA, 1992)
1992	Glioma	3	10	370	Valk[59] (USA, 1992)
	Total*	694			

*It is possible that some patients are represented more than once.

The overall conclusion, based upon the studies summarized above, is that [^{18}F]FMISO PET identifies hypoxic tissue that is heterogeneously distributed within human tumors[93]. It promises to help facilitate image-guided radiotherapy and to also guide the use of hypoxia-selective cytotoxins. These are two of several ways that this agent might help

circumvent the cure-limiting effects of tumor hypoxia. In addition, [^{18}F]FMISO has identified a discrepancy between perfusion, blood-brain barrier disruption, and hypoxia in brain tumors[86] and a lack of correlation between FDG metabolism and hypoxia in several types of malignancies[90]. Hypoxic tissue does not correlate either with tumor volume or vascular endothelial growth factor (VEGF) expression[22,54].

[^{18}F]FMISO PET was able to identify post-radiotherapy tumor recurrence by differential uptake of tracer. The standardized uptake value (SUV) ratio between recurrent tumor and muscle was >1.6, while that between tumor and normal mediastinum was >2.0[60]. One study concluded that [^{18}F]FMISO was not feasible for the detection of tumor hypoxia in human soft tissue tumors[89]. In ischemic stroke, [^{18}F]-FMISO was able to identify the areas of brain tissue into which a stroke had extended[88,92]. In addition to the FMISO imaging studies summarized above, alternative nitroimidazoles have been evaluated as imaging agents in single-center pilot studies. A 2001 study from Finland used [^{18}F]-fluoroerythro-nitroimidazole (^{18}F-FETNIM) to evaluate 8 patients with head and neck squamous cell cancer at doses of ~370 MBq without adverse effect[95] (Lehtio 2001). Other agents, fluoropropyl-nitroimidazole and fluorooctyl-nitroimidazole. have not proved as useful in visualizing hypoxic tissue[96] (Yamamoto 1999), probably because of their higher lipophilicity. A derivative that is more hydrophilic than FMISO, [^{18}F]-fluoroazomycin-arabinofuranoside (FAZA) had been recommended for further study[97] (Sorger 2003) and shows considerable clinical promise.

In human metastatic neck lymph nodes, comparison of FMISO tumor-to-muscle uptake ratio at 2 hours using the computerized polarographic needle electrode system (pO_2 histography) found average to high correlation, whereas no correlation was found with [^{18}F]-2-fluoro-2-deoxyglucose (FDG)[87]. A significant correlation was found between hypoxic tissue identified by FMISO and by immunohistochemical staining for both pimonidazole and carbonic anhydrase IX[98] (Dubois 2004).

Taken together, these imaging studies show that [^{18}F]FMISO is able to identify a unique feature of malignant and endangered tissues, hypoxia, thereby adding to the armamentarium of specific markers used to image tumors and potentially impact treatment for the benefit of individual patients. Low oxygenation status is often phenotypic of tumors that demonstrate a poor response to therapy, which justifies extensive investigation of the utility of agents like [^{18}F]FMISO to improve specific treatment regimens directed at hypoxic tumors.

The rationale for using a T:B ratio of 1.2 to separate normoxia from hypoxia is based on human and animal data. The initial animal results showed that normoxic myocardium ratios were near unity over a wide range of flows. In numerous other organs of normal mice, rats, rabbits and dogs, the mean of the distribution histogram was 1.035, median 0.96, for 1342 samples[99]. Therefore, a cut-off of 1.2 was selected, with confidence that any T:B ratio above that value was indicative of hypoxic tissue. This conclusion is further justified by the human study presented in Figure 7. In this patient with a primary brain tumor, the FDG image was co-registered with the FMISO image (left panel). In brain

regions far from the right frontal tumor, the T:B values for FMISO were uniformly less than 1.2, as depicted by the blue dots in the right panel, even though FDG SUV spanned a range from about 3 to 13. In the tumor area, a substantial fraction of the pixels were still in the normal range, but many values exceeded the cut-off as shown by the colored pixels in the FMISO image. A distribution histogram of the red data points shows a continuous distribution, reflecting the fact that the level of oxygenation is a continuum from normoxic to hypoxic. One consequence of this continuous scale is that FMISO images exhibit only modest contrast. However, the evidence that uptake is independent of blood flow and numerous other physiologic parameters, as described about, provides confidence that FMISO images uniquely identify tumors with prognostically significant levels of hypoxia.

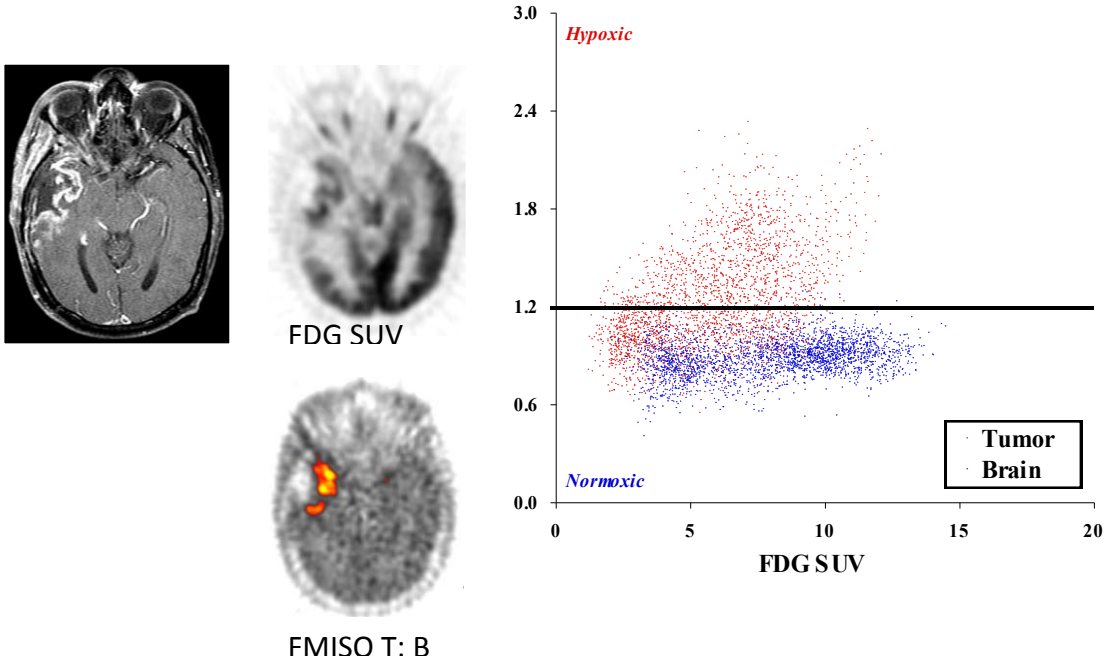

Figure 7. Right-frontal glioma post surgery.

VIII. REFERENCES

[1] Prekeges JL, Rasey JS, Grunbaum Z, and Krohn KH. Reduction of fluoromisonidazole, a new imaging agent for hypoxia. Biochem Pharmacol 1991;42:2387-95.

[2] McClelland RA. Molecular interactions and biological effects of the products of reduction of nitroimidazoles. In*:* Adams GE, Breccia A, Fiedlen EN, and Wardoman P (Eds). NATO Advanced Reserach Workshop on Selective Activation of Drugs by Redox Processes, New York, NY: Plenum Press, 1990. p.125-36.

[3] Brown JM. Therapeutic targets in radiotherapy. Int J Radiat Oncol Biol Phys 2001;49:319-26.

[4] Oswald J, Treite F, Haase C, Kampfrath T, Mading P, Schwenzer B, Bergmann R, Pietzsch J. Experimental Hypoxia is a Potent Stimulus for Radiotracer uptake in Vitro. Cancer Letters 2007; 254: 102-110.

[5] Martin GV, Cerqueira MD, Caldwell JH, et al. Fluoromisonidazole. A metabolic marker of myocyte hypoxia. Circ Res 1990;67:240-4.

[6] Rasey JS, Nelson NJ, Chin L, Evans ML, and Grunbaum Z. Characteristics of the binding of labeled fluoromisonidazole in cells in vitro. Radiat Res 1990;122:301-8.

[7] Rasey JS, Hoffman JM, Spence AM, and Krohn KA. Hypoxia mediated binding of misonidazole in non-malignant tissue. Int J Radiat Oncol Biol Phys 1986;12:1255-8.

[8] Hoffman JM, Rasey JS, Spence AM, Shaw DW, and Krohn KA. Binding of the hypoxia tracer [^{3}H]misonidazole in cerebral ischemia. Stroke 1987;18:168-76.

[9] Piert M, Machulla HJ, Becker G, et al. Dependency of the [^{18}F]fluoromisonidazole uptake on oxygen delivery and tissue oxygenation in the porcine liver. Nucl Med Biol 2000;27:693-700.

[10] Piert M, Machulla H, Becker G, et al. Introducing fluorine-18 fluoromisonidazole positron emission tomography for the localisation and quantification of pig liver hypoxia. Eur J Nucl Med 1999;26:95-109.

[11] Smith BR and Born JL. Metabolism and excretion of [^{3}H]misonidazole by hypoxic rat liver. Int J Radiat Oncol Biol Phys 1984;10:1365-70.

[12] Riedl C, Brader P, Zanzonico Pat, Reid V, Woo Y, Wen B, Ling C, Hricak H, Fong Y, Humm J. Tumor Hypoxia Imaging in Orthotopic Liver Tumors and Peritoneal Metastasis. Eur J Nucl Med Mol Imaging 2008; 35:39-46.

[13] Shelton ME, Dence CS, Hwang DR, et al. In vivo delineation of myocardial hypoxia during coronary occlusion using fluorine-18 fluoromisonidazole and positron emission tomography: a potential approach for identification of jeopardized myocardium [see comments]. J Am Coll Cardiol 1990;16:477-85.

[14] Caldwell JH, Revenaugh JR, Martin GV, et al. Comparison of fluorine-18-fluorodeoxyglucose and tritiated fluoromisonidazole uptake during low-flow ischemia. J Nucl Med 1995;36:1633-8.

[15] Krohn K, Link J, Mason R. Molecular Imaging of Hypoxia. J Nucl Med 2008; 49:129S-148S.

[16] Vallabhajosula S. ^{18}F-Labeled Positron Emission Tomographic Radiopharmaceuticals in Oncology. Semin Nucl Med 2007; 37:400-419.

[17] Wiebe LI and Stypinski D. Pharmacokinetics of SPECT radiopharmaceuticals for imaging hypoxic tissues. Q J Nucl Med 1996;40:270-84

[18] Chapman JD, Franko AJ, and Sharplin J. A marker for hypoxic cells in tumours with potential clinical applicability. Br J Cancer 1981;43:546-50.

[19] Nunn A, Linder K, and Strauss HW. Nitroimidazoles and imaging hypoxia. Eur J Nucl Med 1995;22:265-80.

[20] Franko AJ. Misonidazole and other hypoxia markers: metabolism and applications. Int J Radiat Oncol Biol Phys 1986;12:1195-202.

[21] Wong KH, Wallen CA, and Wheeler KT. Biodistribution of misonidazole and 1,3-bis(2-chloroethyl)-1-nitrosourea (BCNU) in rats bearing unclamped and clamped 9L subcutaneous tumors. Int J Radiat Oncol Biol Phys 1989;17:135-43.

[22] Rajendran JG and Krohn KA. Imaging hypoxia and angiogenesis in tumors. Radiol Clin North Am 2005;43:169-87.

[23] Jerabek PA, Patrick TB, Kilbourn MR, Dischino DD, and Welch MJ. Synthesis and biodistribution of ^{18}F-labeled fluoronitroimidazoles: potential in vivo markers of hypoxic tissue. Int J Rad Appl Instrum [A] 1986;37:599-605.

[24] Grierson JR, Link, J.M., Mathis, C.A., Rasey, J.S., Krohn, K.A. Radiosynthesis of fluorine-18 fluoromisonidazole. J Nucl Med 1989;30:343 - 50.

[25] Grunbaum Z, Freauff SJ, Krohn KA, et al. Synthesis and characterization of congeners of misonidazole for imaging hypoxia. J Nucl Med 1987;28:68-75.

[26] Workman P. Pharmacokinetics of hypoxic cell radiosensitizers: a review. Cancer Clin Trials 1980;3:237-51.

[27] Rasey JS, Grunbaum Z, Magee S, et al. Characterization of radiolabeled fluoromisonidazole as a probe for hypoxic cells. Radiat Res 1987;111:292-304.

[28] Josephy P. Nitroimidazoles. In*:* Anders M, (Ed), Bioactivation of Foreign Compounds, New York: Academic Press, 1985. p.451-83.

[29] Flockhart IR, Sheldon PW, Stratford IJ, and Watts ME. A metabolite of the 2-nitroimidazole misonidazole with radiosensitizing properties. Int J Radiat Biol Relat Stud Phys Chem Med 1978a;34:91-4.

[30] Flockhart IR, Large P, Troup D, Malcolm SL, and Marten TR. Pharmacokinetic and metabolic studies of the hypoxic cell radiosensitizer misonidazole. Xenobiotica 1978b;8:97-105.

[31] Flockhart IR, Malcolm SL, Marten TR, et al. Some aspects of the metabolism of misonidazole. Br J Cancer Suppl 1978c;37:264-7.

[32] Rasey JS, Koh WJ, Grierson JR, Grunbaum Z, and Krohn KA. Radiolabelled fluoromisonidazole as an imaging agent for tumor hypoxia. Int J Radiat Oncol Biol Phys 1989;17:985-91.

[33] Moulder JE and Rockwell S. Hypoxic fractions of solid tumors: experimental techniques, methods of analysis, and a survey of existing data. Int J Radiat Oncol Biol Phys 1984;10:695-712.

[34] Spence AM, Graham MM, Muzi M, et al. Deoxyglucose lumped constant estimated in a transplanted rat astrocytic glioma by the hexose utilization index. J Cereb Blood Flow Metab 1990;10:190-8.

[35] Casciari JJ and Rasey JS. Determination of the radiobiologically hypoxic fraction in multicellular spheroids from data on the uptake of [^{3}H]fluoromisonidazole. Radiat Res 1995;141:28-36.

[36] Koh WJ, Griffin TW, Rasey JS, and Laramore GE. Positron emission tomography. A new tool for characterization of malignant disease and selection of therapy. Acta Oncol 1994;33:323-7.

[37] Whitmore GF, Gulyas S, and Varghese AJ. Sensitizing and toxicity properties of misonidazole and its derivatives. Br J Cancer Suppl 1978;37:115-9.

[38] Brown JM and Workman P. Partition coefficient as a guide to the development of radiosensitizers which are less toxic than misonidazole. Radiat Res 1980;82:171-90.

[39] Stone HB, Sinesi MS. Testing of New Hypoxic Cell Sensitizers in Vivo. Radiat. Res. 1982; 91: 186-198.

[40] Graziano MJ, Henck JW, Meierhenry EF and Gough AW. Neurotoxicity of misonidazole in rats following intravenous administration. Pharmacol Res 33: 307-318, 1996.

[41] Dische S. Hypoxic cell sensitizers in radiotherapy. Int J Radiat Oncol Biol Phys 1978;4:157-60.

[42] Phillips TL, Fu KK. The interaction of drug and radiation effects on normal tissues. Int J Radiat Oncol Biol Phys 1978;4:59-64.

[43] Urtasun RC, Chapman JD, Feldstein ML, Band RP, Rabin HR, Wilson AF, Marynowski B, Starreveld E, Shnitka T. Peripheral neuropathy related to misonidazole: incidence and pathology. Br J Cancer Suppl 1978;37:271-5.

[44] Overgaard J. Clinical evaluation of nitroimidazoles as modifiers of hypoxia in solid tumors. Oncol Res 1994;6:509-18.

[45] Gray AJ, Dische S, Adams GE, Flockhart IR, and Foster JL. Clinical testing of the radiosensitiser Ro-07-0582. I. Dose tolerance, serum and tumour concentrations. Clin Radiol 1976;27:151-7.

[46] Saunders ME, Dische S, Anderson P, and Flockhart IR. The neurotoxicity of misonidazole and its relationship to dose, half-life and concentration in the serum. Br J Cancer Suppl 1978;37:268-70.

[47] Wasserman TH, Phillips TL, Johnson RJ, et al. Initial United States clinical and pharmacologic evaluation of misonidazole (Ro-07-0582), an hypoxic cell radiosensitizer. Int J Radiat Oncol Biol Phys 1979;5:775-86.

[48] Wiltshire CR, Workman P, Watson JV, and Bleehen NM. Clinical studies with misonidazole. Br J Cancer Suppl 1978;37:286-9.

[49] Dische S. Misonidazole in the clinic at Mount Vernon. Cancer Clin Trials 1980;3:175-8.

[50] Dische S, Saunders MI, Flockhart IR, Lee ME, and Anderson P. Misonidazole-a drug for trial in radiotherapy and oncology. Int J Radiat Oncol Biol Phys 1979;5:851-60.

[51] Paget GE. Toxicity tests: A guide for clinicians. In*:* Heinrich AD and Cattell M (Eds). Clinical Testing of New Drugs, New York: Revere Pub. Co, 1965.

[52] Rasey JS, Martin, G.V, Krohn, K.A. Quantifying Hypoxia with Radiolabeled Fluoromisonidazole: Pre-clinical and clinical Studies. In*:* Machulla HJ, (Ed), Imaging of Hypoxia: Tracer Developments, Dordrecht, The Netherlands: Kluwer Academic Publishers, 1999.

[53] Koh WJ, Bergman KS, Rasey JS, et al. Evaluation of oxygenation status during fractionated radiotherapy in human nonsmall cell lung cancers using [F-18]fluoromisonidazole positron emission tomography. Int J Radiat Oncol Biol Phys 1995;33:391-8.

[54] Rajendran JG, Mankoff DA, O'Sullivan F, Peterson LM, Schwartz DL, Conrad EU, Spence AM, Muzi M, Farwell G and Krohn K. Hypoxia and glucose metabolism in malignant tumors: evaluation by [^{18}F]fluoromisonidazole and [^{18}F]fluorodeoxyglucose positron emission tomography imaging. Clin Cancer Res 2004;10:2245-52.

[55] Graham MM, Peterson LM, Link JM, et al. Fluorine-18-fluoromisonidazole radiation dosimetry in imaging studies. J Nucl Med 1997;38:1631-6.

[56] Silverman DH, Hoh CK, Seltzer MA, et al. Evaluating tumor biology and oncological disease with positron-emission tomography. Semin Radiat Oncol 1998;8:183-96.

[57] Rofstad EK and Danielsen T. Hypoxia-induced metastasis of human melanoma cells: involvement of vascular endothelial growth factor-mediated angiogenesis. Br J Cancer 1999;80:1697-707.

[58] Rischin D, Peters L, Hicks R, et al. Phase I trial of concurrent tirapazamine, cisplatin, and radiotherapy in patients with advanced head and neck cancer. J Clin Oncol 2001;19:535-42.

[59] Valk PE, Mathis CA, Prados MD, Gilbert JC, and Budinger TF. Hypoxia in human gliomas: demonstration by PET with fluorine-18-fluoromisonidazole. J Nucl Med 1992;33:2133-7.

[60] Eschmann SM, Paulsen F, Reimold M, et al. Prognostic Impact of Hypoxia Imaging with ^{18}F-Misonidazole PET in Non-Small Cell Lung Cancer and Head and Neck Cancer Before Radiotherapy. J Nucl Med 2005;46:253-60.

[61] Read SJ, Hirano T, Abbott DF, et al. Identifying hypoxic tissue after acute ischemic stroke using PET and ^{18}F-fluoromisonidazole. Neurology 1998;51:1617-21.

[62] Miller RC and Hall EJ. Oncogenic transformations in vitro produced by misonidazole. Cancer Clin Trials 1980; 3: 85-90.

[63] Chin JB, Sheinin DMK, Rauth AM. Screening for the Mutagenicity of Nitro-Group Containing Hypoxic Cell Radiosensitizers Using *Salmonella typhimurium* Strains TA 100 and TA 98. Mutation Research. 1978; 58: 1-10.

[64] Suzanger M, White INH Jenkins TC et al. Effects of Substituted 2-Nitromisonidazoles and Related Compounds on Unscheduled DNA Synthesis in Rat Hepatocytes and in Non-transformed (BL8) and Transformed (JB1) Rat Liver Epithelial Derived Cell Lines. Biochemical Pharmacology. 1987; 36: 3743-3749.

[65] Jung AL, Roan Y, Temple AR. Neonatal death associated with acute transplacental ethanol intoxication. Am J Dis Child. 1980; 134: 419-20.

[66] Szeto MD, Chakraborty G, Hadley J, Rockine R, Muzi M, Alvord EC Jr., Krohn KA, Spence AM, Swanson KR. Quantitive Metrics of Net Proliferation and Invasion Link Biological Aggressiveness Assessed by MRI with Hypoxia Assessed by FMISO-PET in Newly Diagnosed Glioblastomas. Cancer Res 2009; 69: (10).

[67] Swanson KR, Chakraborty G, Wang ChH, Rockne R, Harpold HLP, Muzi M, Adamsen TCH, Krohn KA, Spence AM. Complementary but Distinct Roles for MRI and ^{18}F-Fluoromisonidazole PET in the Assessment of Human Glioblastomas. The J. Nucl Med 2009; 50: (1).

[68] Lee N, Nehmeh S, Schoder H, Fury M, Chan K, Ling CC, Humm J. Prospective Trial Incorporating Pre-/Mid-Treatment [^{18}F]-Misonidazole Positron Emission Tomography for Head-and-Neck Cancer Patients Undergoing Concurrent Chemoradiotherapy. Int. J. Rad Onc Biol Phys.

[69] Spence AM, Muzi M, Swanson KR, O'Sullivan F, Rockhill JK, Rajendran JG, Adamsen TCH, Link JM, Swanson PE, Yagle KJ, Rostomily RC, Silbergeld DL, Krohn KA. Regional Hypoxia in Glioblastoma Multiforme Quantified with [^{18}F] Fluoromisonidazole Positron Emission Tomography before Radiotherapy: Correlation time to Progression and Survival. Clin Cancer Res 2008; 14: (9).

[70] Lin Z, Mechalakos J, Nehmeh S, Schoder H, Lee N, Hum J, Ling CC. The Influence of Changes in Tumor Hypoxia on Dose-Painting Treatment Plans Based on ^{18}F-FMISO Positron Emission Tomography. Int. J. Rad Onc Biol Phys 2008; 70: (4), pp. 1219-1228.

[71] Thorwarth D, Alber M. Individualised Radiotherapy on the Basis of Functional Imaging with FMISO PET. Z. Med. Phys. 2008; 18: pp. 43-50.

[72] Lee N, Mechalakos J, Nehmeh S, Lin Z, Squire O, Cai S, Chan K, Zanzonico P, Greco C, Ling C, Humm J, Schoder H. Int. J. Radiation Onc Biol Phys 2008; Vol. 70 No. 1, pp. 2-13.

[73] Thorwarth D, Soukup M, Alber M. Dose Painting with IMPT, Helical Tomotherapy and IMXT. Radiotherapy & Onc 2008; 86:30-34.

[74] Nehmeh S, Lee N, Schroder H, Squire O, Zanzonico P, Erdi Y, Greco C, Mageras G, Pham H, Larson S, Ling Clifton, Humm J. Reproducibility of Intratumor Distribution of ^{18}F-Fluoromisonidazole in Head and Neck Cancer. Int. J. Rad Onc Biol Phys 2008; Vol. 70, No. 1, pp. 235-242.

[75] Roels S. Slagmolen P, Nuyts J, Lee J, Loeckx D, Maes F, Stroobants S, Penninckx F, Haustermans K. Biological image-guided radiotherapy in rectal cancer. Acta Onc 2008; 47: 1237-1248.

[76] Eschmann SM, Paulsen F, Bedeshem C, Machulla H, Hehr T, Bamberg M, Bares R. Hypoxia-Imaging with ^{18}F-Misonidazole and PE T. Radiotherapy & Oncology 2007; 83:406-410.

[77] Spence A, Muzi M, Link J, Hoffman J, Eary J, Krohn K. NCI Sponsored Trial for the Evaluation of Safety and Prelimanry Efficacy of FLT as a Marker of Proliferation. Mol Imaging Biol 2008, 10:271-280.

[78] Gagel B, Piroth M, Pinkawa M, Reinartz P, Zimny M, Kaiser H, Stanzel S, Asadpour B, Demirel C, Hamacher K, Coenen H, Scholbach T, Maneschi P, DiMartino E, Eble M. pO Polaroghraphy, Contrast Enhanced Color Duplex Sonography (CDS), [^{18}F] Fluoromisonidazole and [^{18}F] Fluorodeoxyglucose Positron Emission Tomography. BMC Cancer 2007; 7:113.

[79] Thorwarth D, Eschmann SM, Paulsen F, Alber M. Hypoxia dose painting by numbers: A planning study. Int. J Rad Onc Biol. Phys. 2007; 68, 1: 291-300.

[80] Zimny M, Gagel B, DiMartino E, Hamacher K, Coenen HH, Westhofen M, Eble M, Buell U, Reinartz P. FDG-a marker of tumour hypoxia? A comparison with [^{18}F] fluoromisonidazole and pO2-polarography. Eur J Nucl Med Mol Imaging 2006 33: 1426-31.

[81] Cherk MH, Foo SS, Poon AMT, Knight SR, Murone C, Papenfuss AT, Sachinidis JI, Saunder THC, O'Keefe JG, Scott AM. Lack of correlation of hypoxic cell fraction and angiogenesis with glucose metabolic rate. J Nucl Med 2006; 47: 1921-26.

[82] Rischin Danny, Hicks R, Fisher R, Binns D, Corry J, Porceddu S, Peters Lester. Prognostic Significace of [^{18}F]-Misonidazole Positron Emission Tomography-Detected Tumor Hypoxia in Patient with Advanced Head & Neck Cancer. J of Clin Onc 2008; 24(13): 2098-2104.

[83] Rajendran JG, Schwartz DL, O'Sullivan J, Peterson LM, Ng P, Scharnhorst J, Grierson JR, and Krohn KA. Tumor hypoxia imaging with [F-18] fluoromisonidazole positron emission tomography in head and neck cancer. Clin Cancer Res 2006; 12(18): 5435-41.

[84] Gagel B, Reinartz P, Demirel C, Kaiser HJ, Zimny M, Piroth M, Pinkawa M, Stanzel S, Asadpour B, Hamacher K, Coenen HH, Buell U, Eble MJ. [^{18}F] fluoromisonidazole and [^{18}F] fluorodeoxyglucose positron emission tomography in response evaluation after chemo-/radiotherapy of non-small-cell lung Cancer: a feasibility study. BioMed Central Can 2006, 6:51: 1-8.

[85] Cher LM, Murone C, Lawrentschuk N, Ramdave Sh, Papenfuss A, Hannah A, O'Keefe GJ, Sachinidis JI, Berlangieri SU, Fabinyi G, Scott AM. Correlation of hypoxic cell fraction and angiogenesis with glucose metabolic rate in gliomas using [^{18}F] fluoromisonidazole, ^{18}F-FDG, PET and Immunohistochemical Studies. J Nucl Med 2006 47: 410-18.

[86] Bruehlmeier M, Roelcke U, Schubiger PA, and Ametamey SM. Assessment of hypoxia and perfusion in human brain tumors using PET with ^{18}F-fluoromisonidazole and ^{15}O-H_2O. J Nucl Med 2004;45:1851-9.

[87] Gagel B, Reinartz P, Dimartino E, et al. pO_2 Polarography versus positron emission tomography ([^{18}F] fluoromisonidazole, [^{18}F]-2-fluoro-2'-deoxyglucose). An appraisal of radiotherapeutically relevant hypoxia. Strahlenther Onkol 2004;180:616-22.

[88] Markus R, Reutens DC, Kazui S, et al. Topography and temporal evolution of hypoxic viable tissue identified by ^{18}F-fluoromisonidazole positron emission tomography in humans after ischemic stroke. Stroke 2003;34:2646-52.

[89] Bentzen L, Keiding S, Nordsmark M, et al. Tumour oxygenation assessed by ^{18}F-fluoromisonidazole PET and polarographic needle electrodes in human soft tissue tumours. Radiother Oncol 2003;67:339-44.

[90] Rajendran JG, Wilson DC, Conrad EU, et al. [^{18}F]FMISO and [^{18}F]FDG PET imaging in soft tissue sarcomas: correlation of hypoxia, metabolism and VEGF expression. Eur J Nucl Med Mol Imaging 2003;30:695-704.

[91] Scott AM, Ramdave S, Hannah A, et al. Correlation of hypoxic cell fraction with glucose metabolic rate in gliomas with [^{18}F]-fluoromisonidazole (FMISO) and [^{18}F]-fluorodeoxyglucose (FDG) positron emission tomography. J Nucl Med 2001;42:678.

[92] Read SJ, Hirano T, Abbott DF, et al. The fate of hypoxic tissue on ^{18}F-fluoromisonidazole positron emission tomography after ischemic stroke. Ann Neurol 2000;48:228-35.

[93] Rasey JS, Koh WJ, Evans ML, et al. Quantifying regional hypoxia in human tumors with positron emission tomography of [^{18}F]fluoromisonidazole: a pretherapy study of 37 patients. Int J Radiat Oncol Biol Phys 1996;36:417-28

[94] Koh WJ, Rasey JS, Evans ML, et al. Imaging of hypoxia in human tumors with [F-18]fluoromisonidazole. Int J Radiat Oncol Biol Phys 1992;22:199-212

[95] Lehtio K, Oikonen V, Gronroos T, et al. Imaging of Blood Flow and Hypoxia in Head and Neck Cancer: Initial Evaluation with [^{15}O]H_2O and [^{18}F]Fluoroerythronitroimidazole PET. J Nucl Med 2001;42:1643-52

[96] Yamamoto F, Oka H, Antoku S, et al. Synthesis and characterization of lipophilic 1-[^{18}F]fluoroalkyl-2- nitroimidazoles for imaging hypoxia. Biol Pharm Bull 1999;22:590-7.

[97] Sorger D, Patt M, Kumar P, et al. [^{18}F]Fluoroazomycinarabinofuranoside (^{18}FAZA) and [^{18}F]Fluoromisonidazole (^{18}FMISO): a comparative study of their selective uptake in hypoxic cells and PET imaging in experimental rat tumors. Nucl Med Biol 2003;30:317-26.

[98] Dubois L, Landuyt W, Haustermans K, et al. Evaluation of hypoxia in an experimental rat tumour model by [(^{18})F]fluoromisonidazole PET and immunohistochemistry. Br J Cancer 2004;91:1947-54.

[99] Rasey JS and Evans ML. Detecting hypoxia in human tumors. In*:* Vaupel P and Jain RK (Eds). Tumor Blood Supply and Metabolic Microenvironment: Characterizations and Implications for Therapy, Funktionanalyze Biologischer Systeme 20: Gustav Fischer Verlag, 1991.